Journal of Applied Electrochemistry (2006) 36:919–929
DOI 10.1007/s10800-006-9150-y
© Springer 2006

Involvement of a metastable surface state in the electrocatalytic, electrodeposition and bath additive behaviour of copper in acid solution

L.D. BURKE[1,*], A.M. O'CONNELL[1,2], R. SHARNA[1] and C.A. BUCKLEY[1]
[1]*Chemistry Department, University College Cork, Cork, Ireland*
[2]*Intel Ireland Ltd, Collinstown Industrial Park, Leixlip, Co. Kildare, Ireland*
*(*author for correspondence, e-mail: l.d.burke@ucc.ie)*

Received 17 January 2006; accepted in revised form 2 May 2006

Key words: bath additives, copper in acid, electrocatalysis, electrodeposition, metastable state

Abstract

Copper in aqueous sulphuric acid solution at room temperature displays a low level active (metastable) surface state redox transition well within the double layer region, at ca. -0.7 ± 0.1 V (SMSE). The latter is an important feature of this electrode system as it apparently coincides with (a) the transition from activation to transport control in acid sulphate copper plating baths, (b) a major change in the inhibiting properties of several plating bath additives, and (c) the onset/termination potential of electrocatalytic processes, e.g. nitrate reduction, at copper in acid. The nature and influence of this active surface state behaviour, which is assumed to be relevant to Damascene copper plating, is discussed.

1. Introduction

The switch from the evaporated aluminium to electrodeposited copper as the technology of choice for on-chip interconnect fabrication in the microelectronic industry has been hailed as "one of the most important changes in materials that the semiconductor industry has experienced since its creation" [1]. Descriptions of this new copper metallization process (also known as Damascene plating) and the advantages of copper, relative to aluminium, have been widely reported [1–5] and need not be repeated here. However, it is worth noting that while the use of a combination of additives in acidified copper sulphate plating baths is crucial (to achieve void-free connectors via superfilling or bottom-up growth during electrodeposition)[5, 6], it is also acknowledged [7–12] that the operation of bath additives is poorly understood. It is assumed here that a more detailed understanding of the mode of operation of such additives will result in improved performance of electrodeposition processes and should thus be of benefit in various areas of technology.

It is well known in metallurgy [13] that electrodeposited copper is a metastable (energy-rich) form of the metal. Evidence of this metastability was provided by recent AFM studies by Buckley and Ahmed [14] which showed that freshly electrodeposited copper, after a significant induction period, undergoes a spontaneous morphological change (SMC). The source of the metastability in the fresh deposit is evidently due to the presence of defects (lattice vacancies, dislocations, grain boundaries, etc.) resulting in the existence of active atoms, i.e. copper atoms with a low lattice stabilization energy.

The importance of defects in surface chemistry is widely acknowledged, e.g. Atkins has pointed out [15] that "defects play an important role in surface growth and catalysis". One of the main objectives of the present work is to extend this idea to copper electrochemistry, i.e. to demonstrate that surface metastability (which entails the presence of surface defects) plays a vital role in the electrodeposition, electrocatalytic and bath additive behaviour in the case of copper in acid solution. The background to Metastable Metal Surface (MMS) states [16] and their role in electrocatalysis was discussed recently for the Gp 11 metals (Au, Ag and Cu) [17–19] and RuO_2 [20]; earlier work on the electrocatalytic properties of copper in base [21, 22], is also worth noting. The essential point is that solid metal surfaces possess two limiting states, designated EMS and MMS (EMS = Equilibrated Metal Surface). While most attention is usually devoted to the low energy EMS state, it is suggested here that in many cases the high energy MMS state (which is both poorly defined and poorly understood) is more important.

2. Experimental details

The main technique used to monitor the electrocatalytic and electrodeposition behaviour of copper in acid

solution was cyclic voltammetry; this was carried out with a computerized electrochemical workstation (CH Instruments, model 660B). A typical copper plating solution [23] contained 0.24 mol dm^{-3} $CuSO_4 \cdot 5H_2O$ (Riedel-de Haën) and 1.80 mol dm^{-3} H_2SO_4 (Merck, 96%); however, in many instances in the present work the $CuSO_4 \cdot 5H_2O$ concentration was reduced to 0.05 mol dm^{-3} (to lower the magnitude of the limiting current). The bath additives involved were thiourea, TU (Aldrich), benzotriazole, BTA (Sigma), polyethylene glycol, PEG, mol. mass 3350 g mol^{-1} (Sigma), diethyl saferine azo dimethyl amine, also known as Janus Green B, JGB (Sigma), bis (3-sulphopropyl) disulphide, SPS (Raschig GmbH) and chloride ions (added as NaCl, Merck); these compounds were added in the form of concentrated stock solutions and only single additive behaviour is described in the present work. Nitrate ions were added to the acid solution in the form of solid sodium nitrate (BDH).

Preliminary work was carried out using copper wire electrodes (ca. 2.0 cm exposed length, 1.0 mm diam., Puratronic grade, Alfa Aesar) sealed directly into soda glass. Whilst this form was retained for the counter electrode in the electrodeposition studies, the working electrode was switched to a rotating disk electrode (RDE) system (EG and G rotator, model 616) which has superior hydrodynamic characteristics. The actual disk used was either platinum or gold (of exposed area ca. 0.2 cm^2) whose surface was regularly cleaned and copper plated before use (typical plating conditions were 10 mA cm^{-2} for 5 sec in 0.05 mol dm^{-3} $CuSO_4$ + 1.8 mol dm^{-3} H_2SO_4 solutions, 500 rpm). A similar copper-plated RDE was used in the electrocatalytic studies and for the latter the counter electrode was gold wire (1.0 mm diam., ca. 2.5 cm exposed length, Puratronic grade, Alfa Aesar) sealed into soda glass. The reference electrode used was saturated mercury/mercury (I) sulphate (SMSE) (Radiometer Analytical) which had a standard potential of 0.641 V (SHE). It was contained in a separate vessel which was connected to the main cell (Metrohm, type EA 876-20) via a Luggin capillary; the latter was used in the usual manner to minimize iR errors due to the potential drop across the electrolytic solution. The cell was usually operated at room temperature, ca. 20 °C.

3. Results

3.1. *The basic electrochemistry of copper in acid solution*

A cyclic voltammogram for a copper wire electrode in aqueous sulphuric acid solution is shown in Figure 1(a). The double layer region extends in this case from ca. −0.45 V to ca. −1.0 V. Anodic current due to copper dissolution commences in the positive sweep just above −0.45 V whilst cathodic current due to hydrogen gas evolution commences in the negative sweep at ca. −1.0 V. These potential values are indicative; onset potentials are assumed to be influenced to some degree by the state of the electrode surface (or the activity of the copper atoms at the latter). Note the absence of an adsorbed hydrogen response; copper (like silver and gold) is a very weak chemisorber; however, despite this, the metal surface (as discussed here later) displays remarkable catalytic activity for certain reactions.

The effect of abrading the copper surface on the cyclic voltammetric response (recorded at high current sensitivity) over the double layer region is illustrated in Figure 1(b). A low level pair of conjugate peaks is evident at ca. −0.7 V which are assumed to be due to a quasi-reversible redox transition of a low coverage active (MMS) state of copper (Cu^*), viz.

$$Cu^+_{surf} + e^- = Cu^* \quad (1)$$

The assignment of this small peak within the double layer region is tentative; it is made mainly by analogy with earlier work on the behaviour of copper in base [21, 22]. What is clear from the work described here later is that this rather ill-defined and poorly understood transition within the double layer for copper in acid is quite significant as it marks the potential for

(i) The transition from activation (or slow discharge) to boundary layer transport (or fast discharge) control in the plating of copper from additive-free acid plating baths.
(ii) The onset (negative sweep)/termination (positive sweep) potential for electrocatalytic processes, e.g.

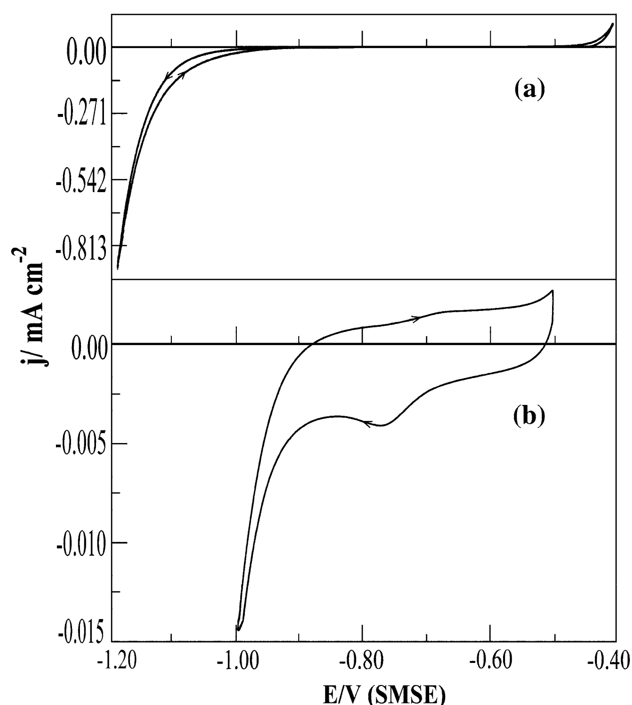

Fig. 1. Cyclic voltammetry responses for (a) an unactivated copper wire electrode (−0.40 to −1.20 V, 5 mV s^{-1}), and (b) the same electrode after subjecting the surface to abrasion with fine grained Emery paper (−0.50 to −1.0 V, 20 mV s^{-1}); in both cases the electrolyte was deoxygenated 1.0 mol dm^{-3} H_2SO_4 at 20 °C.

nitrate ion reduction, at a copper electrode in acid solution.

(iii) The onset of the loss of effectiveness of several plating bath additives, e.g. thiourea, which normally function as inhibitors for copper electrodeposition (such inhibition tends to disappear, in some cases rather dramatically, at ca. −0.7 V).

In essence, this rather nebulous redox transition at ca. −0.7 V often plays a crucial role in the electrochemistry of copper in acid solution (rather similar behaviour, from an electrocatalytic viewpoint, was described recently for gold in acid and base [17] and for both silver [18] and copper [21, 22] in base). The limitations involved in the present work need to be borne in mind, e.g. the species involved in the redox reaction at ca. −0.7 V is assumed to be a low coverage, metastable (or non-equilibrium) state whose precise identity is not known. The potential value for the active state transition (quoted here as −0.7 V) is approximate; it may range from ca. −0.6 V to −0.8 V; also the factors determining this value (or range) are not understood. This element of uncertainty is by no means unique in surface science; surface active sites are among the most important species in chemistry; yet, according to Gates [24] and other authors [25] they remain unidentified and poorly understood.

3.2. *The electrocatalytic properties of copper in acid solution*

Despite its weak chemisorption capability, copper displays excellent catalytic activity for a number of gas phase and electrochemical reactions. The origin of such unexpected behaviour seems to be that copper catalysis [26] involves regenerative, Mars-van Krevelen or surface cyclic redox, rather than activated chemisorption, behaviour. Copper is an excellent catalyst for the water-gas shift reaction and a scheme for repetitive oxidation and reduction of surface (copper) sites (as a vital part of this catalytic process) was outlined by Lloyd and coworkers [26]. The involvement of an unusual copper oxide species, $Cu_{(x\geq10)}O$. as an active site ingredient on copper during the course of partial methanol oxidation at ca. 600 K was established recently by Schedel-Niedrig and coworkers [27]; the species in question was difficult to investigate as it existed only under reaction conditions (it was identified by in situ X-ray absorption spectroscopy).

Copper in aqueous media displays unrivalled electrocatalytic activity for relatively important reactions, e.g. reduction of carbon dioxide to hydrocarbons in base [28, 29] and the reduction of nitrate ions [30–32] in acid solution. It is again assumed that, as in the case of the copper-catalyzed gas phase reactions, an interfacial cyclic redox (or surface mediator) route for reaction is involved. This mediator route for electrocatalysis was discussed earlier [21, 22] for copper in base and an equivalent scheme for nitrate ion reduction to ammonia [30] in acid solution may be summarized as follows, viz.

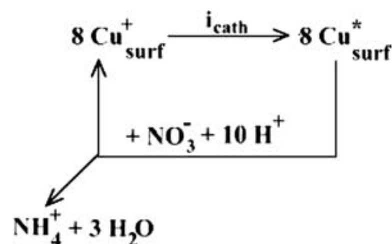

Support for the assumption that an active (MMS) surface state of copper is involved in the nitrate reduction reaction is provided by the response for this process shown by the dashed line in Figure 2. The responses for the negative and positive sweep were very similar; virtually no reduction was observed over the range −0.4 to −0.6 V. Below the latter value, where the $Cu^{*}/Cu^{+}{}_{surf}$ couple is assumed to become involved, the rate of reduction increased (though not very rapidly) with decreasing potential until a plateau value was attained at ca. −1.1 V. For a fixed nitrate ion concentration (0.05 mol dm^{-3}) the rate of reduction in the plateau region increased significantly (Figure 3) with increasing rotation rate and the data obtained yielded a linear Levich plot (Figure 4) which gave an intercept (at $\omega^{1/2}=0$) close to, but not quite, zero ($j_L[\omega^{1/2}=0]=5.7$ mA cm^{-2}). It is assumed here that the limiting current for nitrate ion reduction at copper in acid is determined largely by boundary layer transport of NO_3^- ions. Quite high rates of nitrate reduction were observed, Figure 5, the limiting (or plateau) values being a linear function of the nitrate ion concentration, at least to values of the latter up to 0.3 mol dm^{-3}.

Two points about the nitrate ion reduction at copper in acid are worth noting: (i) the rate of increase in current density with decreasing potential is sluggish (Figure 3) (at high nitrate concentration, and consequently high reduction rates, the onset of the plateau region overlapped with

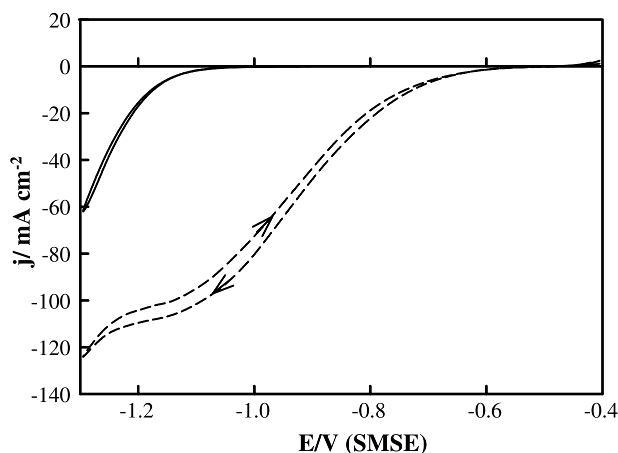

Fig. 2. Cyclic voltammograms (−0.4 to −1.3 V, 10 mV s^{-1}) for a copper-plated RDE (500 rpm) in deoxygenated 1.0 mol dm^{-3} H_2SO_4 without (full line) and with (dashed line) 0.05 mol dm^{-3} NO_3^- present; T = 20 °C.

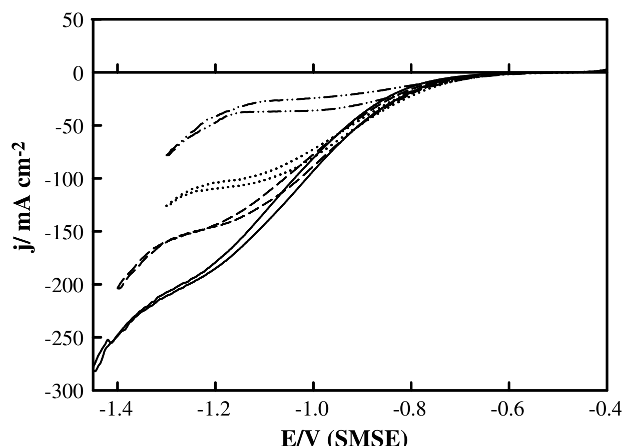

Fig. 3. Effect of electrode rotation rate on the CV responses for a copper plated RDE in acidified 0.05 mol dm^{-3} nitrate solution; the conditions involved are described in Figure 2 except that at higher rotation rates the lower limit of the sweep was extended to more negative values: –··–, 50 rpm; ..., 500 rpm; - - -, 1000 rpm; —, 2000 rpm.

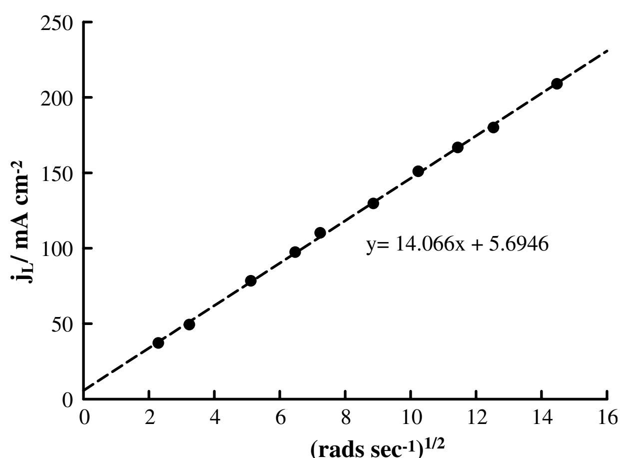

Fig. 4. Levich plot for the nitrate reduction process at a copper plated RDE electrode in acid solution; same conditions as in Figures 2 and 3; j_L is the limiting (or plateau) value.

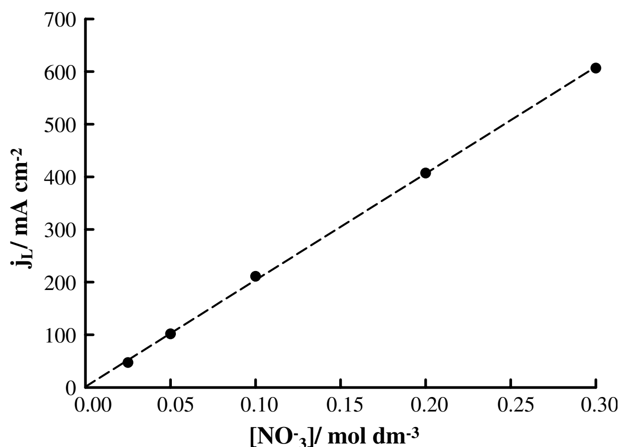

Fig. 5. Variation of the limiting current density for nitrate reduction on copper with NO_3^- concentration in 1.0 mol dm^{-3} H_2SO_4; similar conditions as in Figure 2.

the hydrogen gas evolution response); (ii) the rate of nitrate reduction at a fixed potential decreased gradually with time (from ca. 31 to 17 mA cm^{-2} over a period of 30 min: $[NO_3^-]$ = 0.1 mol dm^{-3}, $E = -0.8$ V). The reduction of other species, e.g. dissolved oxygen gas and nitrobenzene (the solvent used for the latter was a mixture of 50% water + 50% isopropanol (v/v) [33]) was also investigated. As with nitrate, reduction commenced in both cases at copper in acid solution at ca. −0.6 V (a detailed account of the latter work will be published later); the important point is that the onset potential for reduction for the three species is virtually independent of the nature of the dissolved reactant; it is determined by the redox transition of the MMS (or Cu^*/Cu^+_{surf}) couple.

A comparison was also made of reduction responses for nitrate on copper in sulphuric acid and perchloric acid solution. As illustrated in Figure 6, the trends were very similar but the onset potential was lower in $HClO_4$ (ca. −0.55 V) as compared with H_2SO_4 (ca. −0.65 V). The onset potential for reduction was difficult to assess accurately as the increase in current with decrease in potential was quite slow. However, for the conditions outlined in Figure 6 the half-wave potential for nitrate reduction was ca. −1.015 V in H_2SO_4 and ca. −0.925 V in $HClO_4$ solution.

3.3. *The electrodeposition of copper in additive-free acidic copper plating baths*

Typical examples of responses for a copper surface in a sulphate plating bath are shown in Figure 7. In each case there was a switch from copper dissolution to copper deposition at ca. −0.4 V. In part (a), where no electrode rotation was employed, the cathodic response below −0.4 V in the negative sweep was abnormally large; in the absence of stirring the boundary layer is quite thick and at −0.4 V contains an unusually high concentration of Cu^{2+} ions produced anodically at the beginning of the negative sweep (where the metal

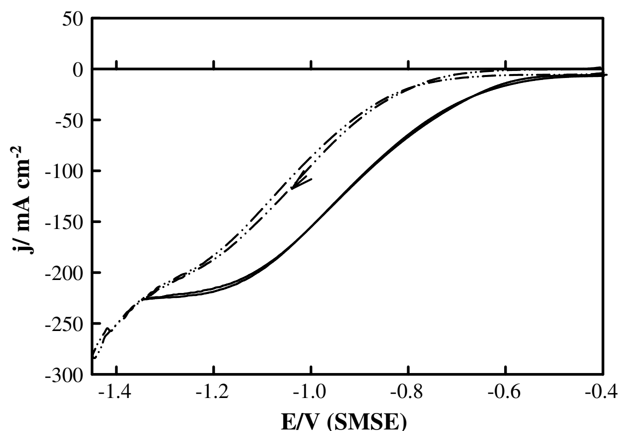

Fig. 6. Comparison of the nitrate reduction response at copper ($v = 10$ mV s^{-1}; $[NO_3^-]$ = 0.05 mol dm^{-3}) in 1.0 mol dm^{-3} H_2SO_4 (broken line) and 1.0 mol dm^{-3} $HClO_4$ (full line); conditions otherwise were as in Figure 2.

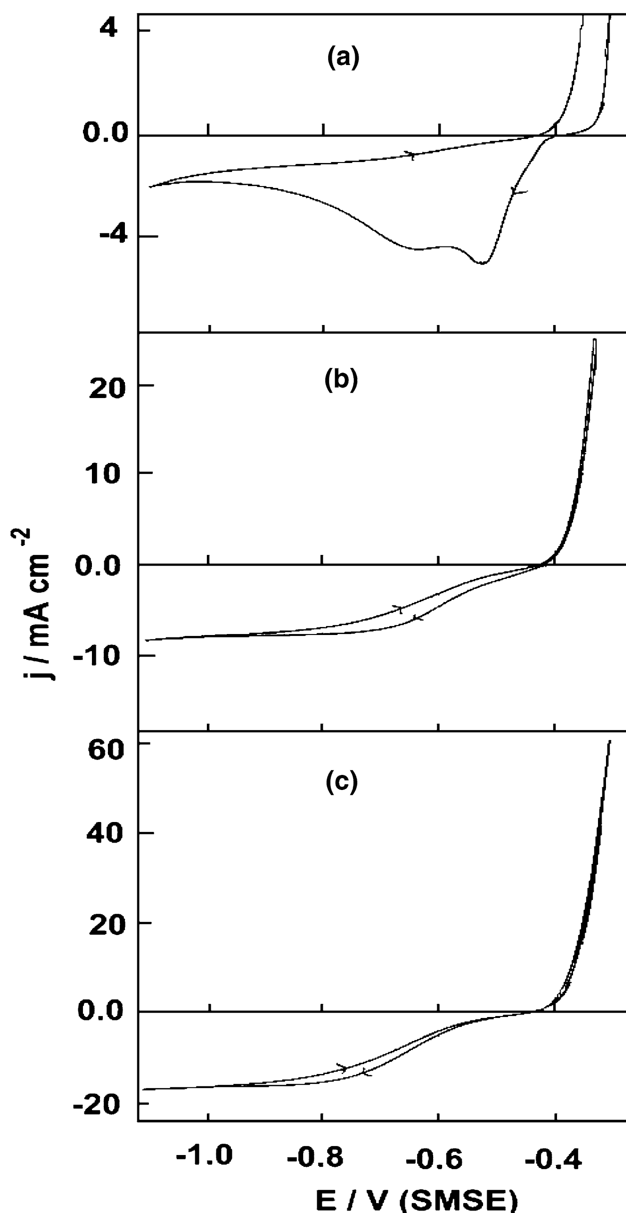

Fig. 7. Cyclic voltammograms (−0.35 to −1.1 V, 20 mV s^{-1}) for a copper plated RDE in 1.8 mol dm^{-3} H_2SO_4 + 0.05 mol dm^{-3} $CuSO_4$ at 20 °C: (a) 0 rpm, (b) 100 rpm, (c) 500 rpm.

undergoes vigorous dissolution). The responses shown in (b) and (c) are typical for electrode rotation conditions of 100 and 500 rpm, respectively: the anodic response rose dramatically with increasing potential above −0.4 V, while the cathodic response (below the latter value) was quite sluggish initially but reached a diffusion-controlled limiting value at ca. −0.75 V. The limiting (or plateau) current density values increased significantly with increasing electrode rotation rate and Levich plot data, Figure 8, confirmed boundary layer diffusion control. Diffusion coefficient values (D/ cm^2 s^{-1}) estimated for Cu^{2+} ions in 0.01, 0.05 and 0.24 mol dm^{-3} $CuSO_4$ (plus 1.80 mol dm^{-3} H_2SO_4) were 7.16× 10^{-6}, 9.19× 10^{-6} and 8.47× 10^{-6}, respectively; these are in reasonable agreement with previously reported [34] data for this parameter which range from

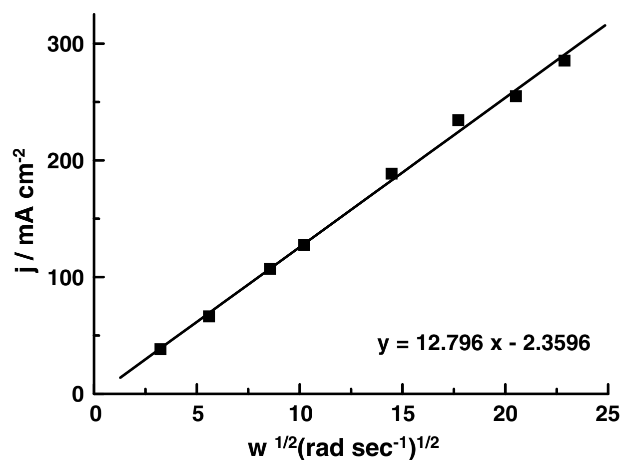

Fig. 8. Levich plot for copper electrodeposition in 1.8 mol dm^{-3} H_2SO_4 + 0.24 mol dm^{-3} $CuSO_4$ at 20 °C; rate values were taken at the lower limit in sweeps recorded under the conditions outlined in Figure 8.

5.4× 10^{-6} to 9.7× 10^{-6} cm^2 sec^{-1}. Tafel plots, based on the type of voltammetric responses shown here in Figure 7(b), yielded Tafel slopes of ca. 46 and −120 mV $decade^{-1}$ for the dissolution and deposition reaction, respectively. Obviously this Tafel slope value in the case of electrodeposition relates to the activation (or slow discharge), $E > -0.7$ V, region of the curve (severe deviation from linearly in the case of the Tafel plot for deposition was observed at $E < -0.6$ V).

Deposition responses for sulphate and perchlorate solutions are compared in Figure 9. Very similar trends were observed, the rate at a given potential was slightly faster in the perchlorate solution, but in both cases the switch from activation to transport control occurred at ca. −0.75 V. The transport control limiting values were appreciably higher in the perchlorate solution (this was confirmed for cases where the initial copper electrodeposit was produced in the same, sulphate or perchlorate, solution).

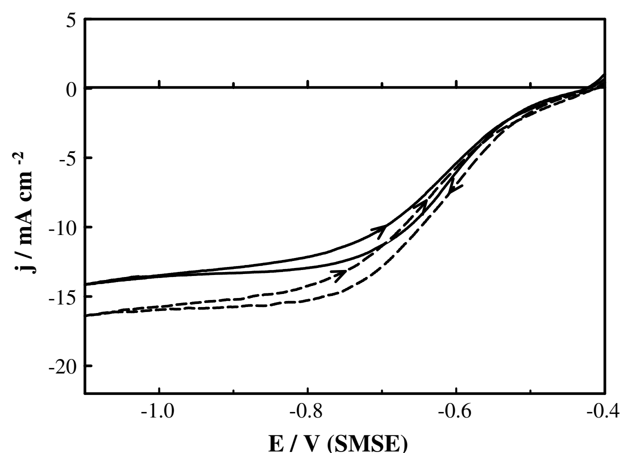

Fig. 9. Comparison of the response (−0.40 to −1.10 V, 20 mV s^{-1}) for copper electrodeposition at a copper plated RDE (400 rpm) in 1.8 mol dm^{-3} H_2SO_4 + 0.05 mol dm^{-3} $CuSO_4$ (full line) and in 1.8 mol dm^{-3} $HClO_4$ + 0.05 mol dm^{-3} $Cu(ClO_4)_2$ (dashed line), T = 20 °C.

3.4. *Effect of plating bath additives*

(a) Thiourea (and BTA): Responses for copper electrodeposition without (full line) and with (dashed line) a low concentration (10 ppm) of thiourea in the plating bath are shown in Figure 10(a). It is clear that thiourea has a severely inhibiting effect on the plating reaction; however, in the negative sweep there was a dramatic increase in plating rate at ca. −0.8 V. At this relatively low concentration of the additive the inhibition of the plating process in the positive sweep occurred in a less dramatic manner. On increasing the additive concentration, Figure 10(b), the responses for the negative and positive sweep were very similar; the inhibition of the plating reaction in both cases was quite severe over the range −0.4 to −0.8 V and the switchover to rapid plating (at or below −0.8 V, negative sweep) was rather sluggish. The presence of thiourea also seemed to catalyse the hydrogen gas evolution reaction at $E < -1.1$ V; however, this aspect of thiourea behaviour was not investigated in detail. The effect of BTA (as sole additive) was very similar to that of thiourea; its effect on the copper plating process will be described in more detail later.

(b) Chloride ion: Chloride ions generally act as an accelerator or catalyst for copper deposition in acid sulphate plating baths [5] and the effect, for 50 ppm Cl^-, is illustrated here in Figure 11. It is clear from the responses shown in the latter that the copper deposition rate is much faster in the presence of chloride ion over the activation controlled plating region, i.e. from −0.40 to −0.75 V. The chloride ion have little effect on the plating rate at $E < -0.75$ V as in this region the reaction rate is limited mainly by boundary layer transport.

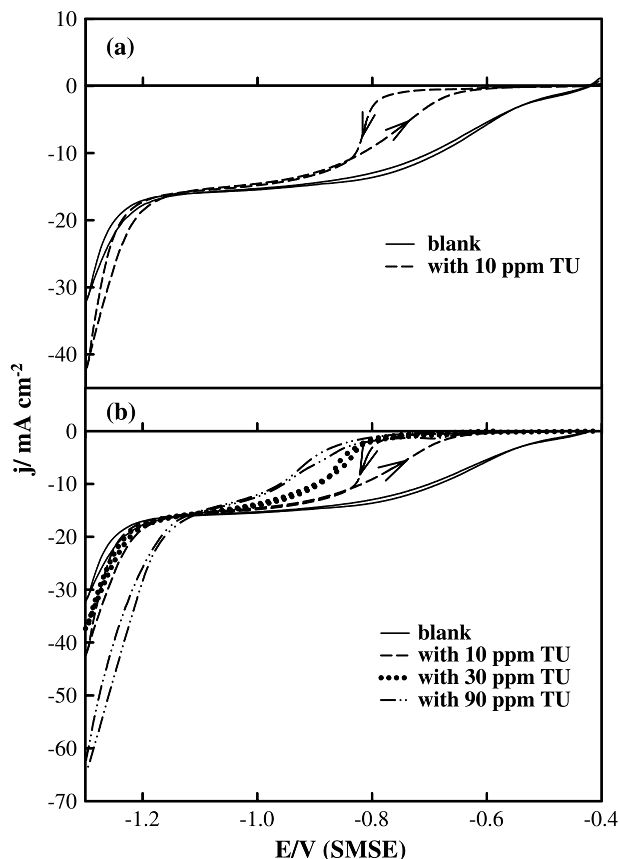

Fig. 10. Effect of addition of different levels of thiourea (TU) on the copper electrodeposition response under CV conditions (−0.40 to −1.30 V, 10 mV s^{-1}); 1.0 mol dm^{-3} H_2SO_4 + 0.05 mol dm^{-3} $CuSO_4$, Cu-plated RDE (500 rpm); T = 20 °C: TU conc. (ppm):- (a) —, 0; - - -, 10: (b) —, 0; - - -, 10; ..., 30; –··–, 90.

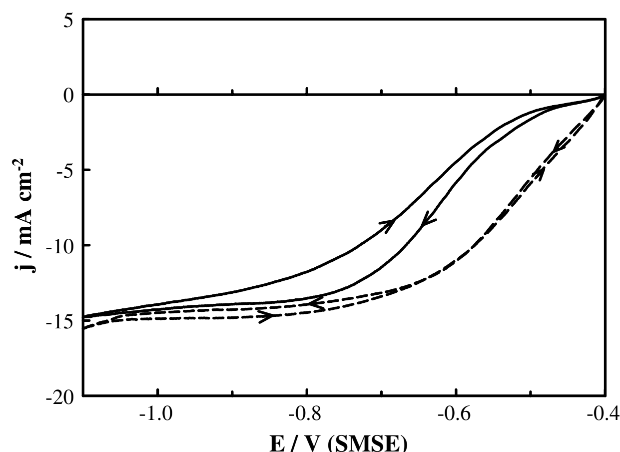

Fig. 11. Cyclic voltammograms (−0.40 to −1.10 V, 20 mV s^{-1}) for a Cu-plated RDE in 0.05 mol dm^{-3} $CuSO_4$ + 1.8 mol dm^{-3} H_2SO_4 at 20 °C: full line, no additive; dashed line, 50 ppm Cl^-.

(c) PEG + Chloride ions: When used as a sole additive, PEG had little effect on the rate of copper deposition under CV conditions, i.e. the response shown for the absence of additive in Figure 12 (the full line) is similar to that observed in the presence of PEG. A very different response was observed, dashed line in Figure 12, when the combination of additives, PEG (300 ppm) and Cl^- ions (50 ppm), was present in the solution. Severe inhibition of the electrodeposition reaction was observed over the range −0.4 to −0.7 V but below this range, at $E < -0.7$ V, the plating current

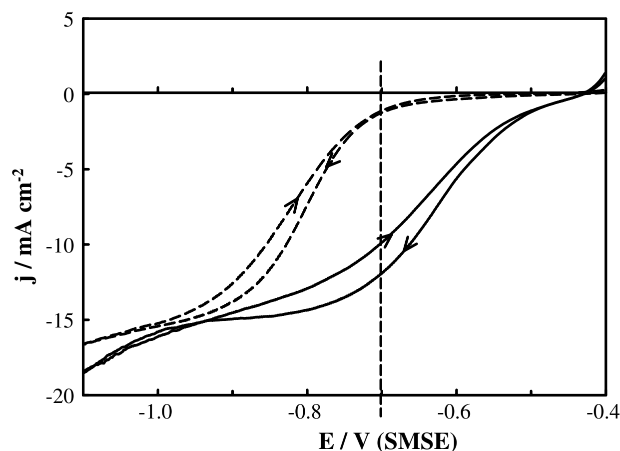

Fig. 12. Cyclic voltammograms recorded under the same conditions as in Fig. 11; again, the full line is the blank (no additive present), whereas the broken line is the response recorded in the presence of 300 ppm PEG + 50 ppm Cl^-.

increased dramatically with decreasing potential to reach a limiting, transport controlled, value below ca. −0.9 V. The vertical dashed line in this case, at ca. −0.7 V, is included here to highlight the fact that whereas in the absence of the additives the plating process approaches its limiting rate value at this potential, the plating rate in the presence of the PEG + Cl^- combination is just about to commence its initial rapid increase at ca. −0.7 V (similar behaviour was observed, in the negative sweep, in the presence of JGB, Figure 13).

(d) Effect of JGB (and SPS): The effect of adding a low level (1 ppm) of JGB to the plating bath is illustrated by the dotted line in Figure 13. JGB acted as an inhibitor, at least down to ca. −0.7 V, in the negative sweep but this inhibition in the activation controlled region was virtually absent in the positive sweep. The trend was rather similar to that observed with a low level of thiourea, see Figure 10(a); however, this difference in character between the negative and positive sweep was maintained in the presence of JGB, even at concentration values of 50 ppm, whereas with higher levels of thiourea, e.g. 30 ppm, the responses for the negative and positive sweeps virtually coincided. Addition of SPS (as sole additive; 1 ppm) to the plating bath had little effect on the copper electrodeposition (CV) response in the negative sweep (dashed line in Figure 13). In the positive sweep the presence of SPS reduced the plating rate over the entire range of the scan.

4. Discussion

4.1. *Active states of metal surfaces*

Defects in the form of kinks, steps and dislocations, are present at all real solid metal surfaces, even those of a clean and well-defined character [35]. Since the work of Taylor [36] in 1925, it has generally been accepted that metal atoms at such sites, which usually constitute only a low percentage of the total number of surface atoms, are often the main centres of surface reactivity, especially from a catalytic viewpoint. In a review of this topic, Somorjai [37] highlighted the diversity of active site atoms (terrace adsorbed, step adsorbed, kink, ledge and terrace embedded atoms), which differ in the number of nearest neighbours, lattice stabilization energy (and hence chemical potential), number of coordination sites exposed to the adjacent fluid phase, adsorption energy for reactants, etc. It seems that the operation of a catalytic surface can be quite complex; for some reactions the active site atoms are highly localized, protruding atoms or subnanoclusters, the vast majority of surface atoms being spectator species [24]. For other reactions (at the same surface) a more extensively coordinated, lower energy, cluster or terrace site may be involved. One of Somorjai's main conclusions is that surface active sites, based on surface irregularities, are strongly influenced by local atomic structure (or disorder), local composition (which may well include subsurface oxygen [27]) and local bonding between adsorbates and surface sites.

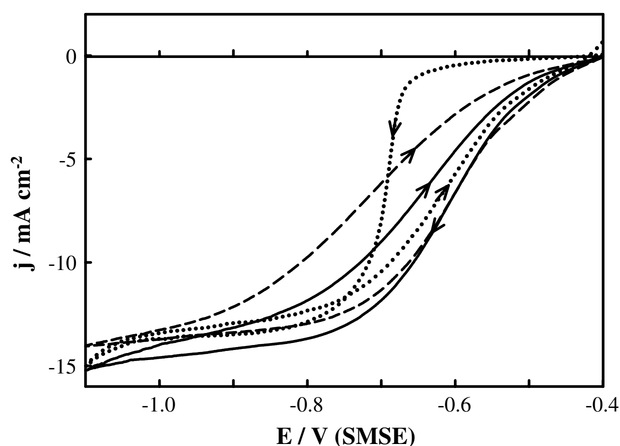

Fig. 13. Cyclic voltammograms recorded under the same conditions as in Figure 11; the full line is the blank (no additive present), whereas the dashed and dotted lines were recorded following addition of 1 ppm SPS and 1 ppm JGB, respectively.

An important factor in surface disorder highlighted by Somorjai [37] is that protruding surface atoms tend to exist in a cationic state, i.e. such atoms tend to lose free electrons to the underlying bulk metal lattice. Support for such behaviour is provided by the theoretical work of Kesmodel and Falicov [38], and is in agreement with conclusions based on studies of the properties of metal microclusters (M_n) in aqueous media by Henglein [39] (according to latter, the oxidation potential of a cluster drops dramatically as the number atoms present is reduced to extremely low values). This has important implications from an electrochemical viewpoint as it means that active site metal atoms undergo oxidation at unusually low potentials and this evidently is the basis of premonolayer oxidation phenomena [40]. Conversely, it means that metal ion discharge will be inhibited at low cathodic overpotentials unless the resulting metal atoms can simultaneously increase their lattice coordination numbers and lattice stabilization energies.

According to Somorjai [37], the ionized metal atom at a corner site is surrounded by a large local electric field which tends to polarize incoming molecules and rupture bonds in the latter. However, at a metal/aqueous solution interface this localized field will attract anions (OH^- or X^-), or expel protons from coordinated water molecules. As the active atom is a protruding species, the resulting ions can coordinate an unusual number of ligands; hence, as outlined recently for gold [17], the product of premonolayer oxidation tends to be a hydrous (β), rather than the normal monolayer (α), oxide species.

It is worth bearing in mind also that there are two modes of electrocatalysis at metal/solution interfaces. The first is activated chemisorption [41] and is well

known for platinum; in this case the active site atom does not normally undergo a redox transition as part of the electrocatalytic process. The second mechanism is the interfacial cyclic redox or IHOAM (Incipient Hydrous Oxide/Adatom Mediator) route [17, 40], and is the equivalent, in heterogeneous catalysis, of the Mars-van Krevelen [26] mechanism. This cyclic redox route is assumed to be of major importance with regard to the electrocatalytic behaviour of Au [17], Ag [18] and Cu [19], which are very weak chemisorbers, and also in the chemically modified electrode area [42]. Its application to catalysis at metal surfaces presents interesting theoretical challenges as non-equilibrium states of matter are involved, i.e. both the oxidized and reduced form of the interfacial couple are thermodynamically unstable at the potential where the active state redox transitions and associated electrocatalytic reactions occur.

4.2. *Active site and electrocatalytic behaviour of copper*

As discussed earlier [16], solid metals and their surfaces can store energy via defect formation. The defect states involved are thermodynamically unstable, but they persist for quite long times; indeed low coverage defects are assumed to be a permanent feature of real solid surfaces. In the absence of prior surface activation, the redox behaviour of active site atoms is often undetectable, as in the case of Figure 1(a) where the double layer response is featureless. Disrupting the surface by abrasion raises the coverage of the active state and leads to the appearance of a low level redox response for the latter at ca. −0.7 V, Figure 1(b).

Copper is a very weak chemisorber, as demonstrated but the absence in Figure 1 of any indication of an adsorbed hydrogen response. Hence, an interfacial cyclic redox (see Eqn. 2), rather than an activated chemisorption, route for catalysis is assumed to be involved in the case of nitrate reduction at copper in acid. The precise nature of the mediating couple, and why the transition occurs at ca. −0.7 V, have yet to be established (as mentioned by Somorjai, there is much scope for theoretical calculations in this area). The nitrate reduction current begins to increase below ca. −0.6 V, Figure 2, i.e. well within the double layer region, but the cathodic response increases in a rather sluggish manner with increasing negative potential, i.e. some step of the overall cathodic reaction is not very facile. However, limiting rates of reaction were observed at different electrode rotation rates (Figure 3) and the Levich plot (Figure 4) demonstrates that the maximum rate of nitrate reduction at copper in acid at low potentials is limited (as least initially) by boundary layer transport of nitrate ions.

Superficially, nitrate ion reduction at copper in acid solution appears to be a relatively simple process, the limiting rate of reaction under potential sweep conditions, Figure 5, being proportional to the bulk concentration of the reactant (as expected for a transport controlled process). However, the rate of reduction at constant potential decays significantly with time; such decay in activity of copper cathodes, especially in base, has been observed by other authors [29]. It is assumed here that this loss of performance is due to the gradual loss of surface active states or sites which are intrinsically unstable. In practice this loss in activity with time may be partly counteracted either by replating the surface with fresh copper [31] or by disrupting the copper surface at regular intervals on application of intermittent anodic pulses [29]; an important point here is that loss of performance is not necessarily due to adsorption of a deactivating impurity or side-product. The data shown in Figure 6 demonstrates that the reaction rate is influenced by the nature of the electrolyte; sulphate and bisulphate anions evidently interact more strongly (presumably with the oxidized form of the mediator system, Cu^{+}_{ads}) than perchlorate. Either the mediator transition potential is shifted to more negative potentials or the rate of the interfacial cyclic process is impeded by the presence of sulphate; the net effect is that over the range of ca. −0.6 to −1.3 V, under the conditions outlined in Figure 6, the rate is lower (at a given potential) in H_2SO_4, as compared with $HClO_4$, solution.

4.3. *Electrodeposition of copper*

It is well known that there is usually a nucleation barrier which inhibits the deposition of metal ions at low cathodic overpotentials at a metal/aqueous solution interface. Such inhibition may be attributed to high energy of copper atoms deposited at terrace sites at the electrode surface, viz.

$$Cu^{2+}(aq) + 2e^{-} = Cu^{*} \quad (3)$$

The energy of the atoms (Cu*) deposited at such sites is high due to their severe lack of lattice stabilization energy; indeed it is most unlikely that high energy states, e.g. copper adatoms, can be produced at appreciable rates at terrace sites. Discharge of copper ions at the interface occurs more readily at surface defect sites, e.g. at steps and kinks, where the product is most likely to be stabilized and, as some of these defects, e.g. spiral dislocations, do not disappear [43], the discharge of copper continues. Direct STM evidence for the involvement of surface defects in the initial stages of metal electrodeposition processes has been reported by Kolb and coworkers [44].

Electrodeposited copper is well known [13] to be an active state of the metal, i.e. some of the metal atoms present exist in metastable (Cu*) states. The precise identity of these states and their distribution within the solid, and especially at the surface, are unknown but their coverage in the nascent deposit is likely to be high (and is assumed to decay gradually as the deposit ages). As discussed here earlier, active copper atoms are likely to be ionized, see Eqn. (1), at $E > -0.7$ V, and this

appears to be the reason why copper ion discharge is sluggish, (b) and (c) in Figure 7, above ca. −0.7 V. The source of inhibition is assumed to be the presence of Cu^{+}_{ads} ions which repels Cu^{2+} (aq) ions at the interface. The positive ions at the interface may arise in two ways, (a) partial discharge of Cu^{2+} ions and/or (b) ionization of active copper atoms, viz.

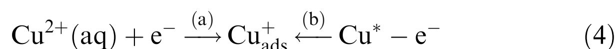

$$Cu^{2+}(aq) + e^{-} \xrightarrow{(a)} Cu^{+}_{ads} \xleftarrow{(b)} Cu^{*} - e^{-} \quad (4)$$

Below −0.70 V the Cu^{+}_{ads} state is reduced to active copper, Cu*, see Eqn. (1), and hence the barrier to Cu^{2+} ion reduction disappears and the plating rate becomes transport limited (see Figure 8). The electrodeposited copper produced in this region is still energy-rich or metastable, but the surface layer at $E <$ ca. −0.7 V now consists predominantly of neutral copper atoms.

The same trends discussed here for copper deposition in sulphate solution were observed also in perchlorate solution, Figure 9. The slightly higher value for the limiting current density observed for the perchlorate system is evidently due to a slightly faster rate of Cu^{2+} transport in the latter case.

The kinetics of copper deposition in acid solution were investigated by Mattson and Bockris [45]. While they interpreted their results in a conventional manner (two successive 1-electron transfer reactions, the first being rate limiting), they also pointed out some complications in the system, e.g. overpotentials recorded for constant current pulses did not always show clear steady-state values, and exchange current density (j_0) values (for the same experiment) obtained from linear j/E plots differed from those derived by extrapolation of Tafel plots. Evidently the metastability of the intermediates and products affects the kinetics of copper deposition.

4.4. *Effect of bath additives*

Thiourea (TU) is a well known inhibitor for copper deposition in acid copper plating baths [46–48] and this additive forms a series of complexes, $Cu(TU)^{+}_{x}$, with Cu(I) cations [49]. It is assumed here that the formation of Cu^{+}_{ads} ions at the interface, Eqn. (4), at the start of the plating reaction results, in the presence of thiourea, in the formation of some adsorbed Cu(I)-thiourea complexes. The latter severely inhibit copper ion deposition at the early stages (−0.45 to −0.70 V) of the negative sweep, Figure 10(a), but below ca. −0.8 V this inhibition disappears, evidently due to the absence in this region of Cu^{+}_{ads} species (which at this stage are reduced to Cu* atoms). In the subsequent positive sweep marked inhibition of the copper deposition reaction recommences as the potential approaches −0.8 V as at this stage Cu^{+}_{ads} ions begin to reappear at the electrode surface. The range of inhibition seems to extend slightly in the negative direction with increasing thiourea concentration, Figure 10(b). This is probably due to the greater stability of the surface complex, $Cu(TU)^{+}_{x,ads}$, with respect to reduction as the activity of the ligand is increased.

Chloride ion is a well known accelerator for the plating reaction in acid copper baths [5]: as shown here in Figure 11 the plating rate is much faster at low overpotentials when chloride ions are present. Without this additive, Cu^{+}_{ads} ions (as discussed here earlier) are produced at the interface and these acts as an electrostatic barrier to further Cu^{2+} discharge. Chloride ions evidently reduce the height of this barrier, probably by bonding to the adsorbed cation species, viz.

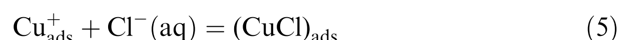

$$Cu^{+}_{ads} + Cl^{-}(aq) = (CuCl)_{ads} \quad (5)$$

i.e. the positive charge (or field) at the metal side of the interface is largely neutralized, the electrostatic barrier is greatly reduced, the major source of inhibition disappears and the plating rate at $E > -0.6$ V becomes much faster. It is possible also that the chloride ions significantly alter the nature of the electrode, converting the latter (at least at the more active regions of the surface) from a metal/metal ion to a metal/insoluble salt system. The main discharge reaction in the presence of Cl^{-} ions may be represented as

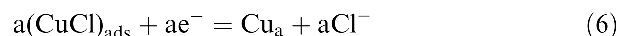

$$a(CuCl)_{ads} + ae^{-} = Cu_{a} + aCl^{-} \quad (6)$$

i.e. copper clusters (Cu_a), rather that copper atoms (Cu*) are produced and the former (being of lower activity, especially if magic number clusters [39] are involved) are much less likely to re-ionize, i.e. the rate of discharge is assumed to be faster in the presence of Cl^{-} as (i) the height of the activation energy barrier is reduced and (ii) the copper species produced in the initial stage of the discharge reaction are of lower energy. Nagy and coworkers [50] attributed the catalytic effect of Cl^{-} ions in the copper plating process to the ability of these ions to alter the discharge process from a sluggish outer-sphere to a faster inner-sphere, chloride bridge, mechanism.

PEG is a relatively large molecule which, in the absence of chloride ions (and as sole additive at a level of 300 ppm), had only a slight inhibiting effect on the plating rate in the activation controlled region. However, when PEG is present along with chloride ions the inhibition effect in the region in question is quite severe, Figure 12. The additive effect of PEG + Cl^{-} ions is similar to that of thiourea (Figure 10) in that the plating process is strongly suppressed until the potential drops below ca. −0.7 V, i.e. until Cu^{+}_{ads} ions disappear from the interface. The role of PEG plus chlorine ions as additives has received much attention [23, 51–55]; it was suggested by Healy and coworkers [52] that complexes such as $Cl–Cu^{I}$-PEG and $Cl–Cu^{II}$-PEG form an inhibiting layer on the copper surface at low overpotentials. The low degree of inhibition at more negative overpotentials was attributed to the absence of Cl^{-}_{ads} at $E <$ the potential of zero charge, plus the inability of PEG molecules to bind strongly to the copper surface. It certainly seems that Cl^{-} ions are

essential for strong PEG adsorption, the important species in this case being $CuCl_{surf}$, which may be partially hydrated, or a copper cluster derived from same. The reduction of the active state, Cu^{+}_{surf},, at ca. −0.7 V results in loss of both the $CuCl_{surf}$ state and the inhibiting PEG species.

The response recorded on adding JGB to the plating bath, Figure 13, was somewhat unusual. Severe inhibition was observed in the negative sweep until ca. −0.7 V; similar behaviour was observed on adding thiourea (Figure 10) and PEG + Cl^- ions (Figure 12). However, much less inhibition was observed over the activation region ($E > -0.7$ V) of the positive sweep in the presence of JGB; indeed the plating rate above −0.7 V in the positive sweep was slightly larger with JGB present than in the absence of this additive (Figure 13). It may be noted that similar, but less dramatic, behaviour was observed in the presence of a low level of thiourea, Figure 10(a), i.e. the plating rate above −0.8 V was somewhat faster in the positive, as compared to the negative, sweep. The origin of such a difference is currently unclear; it may due to a slow complexation reaction. Possibly more of the inhibiting species (Cu^+/JGB complex) is formed at the beginning of the negative sweep where the plating rate is quite low, and much of this inhibiting film is retained until the potential drops below ca. −0.7 V. At the beginning of the positive sweep there is no Cu^{+}_{ads} species at the surface and hence no inhibiting complex. The latter should begin to appear at the surface in the positive sweep at ca. −0.7 V but if the rate of complexation is slow plating can continue without severe inhibition at a rate similar to that observed in the absence of the additive. This aspect of the effect of JGB requires further investigation.

5. Conclusions

1. Low coverage, high energy, metastable atoms are regarded as the basis of active site behaviour at metal electrode surfaces. Such atoms undergo cyclic redox transitions, as a vital component in many electrocatalytic reactions (as outlined recently for gold [17]), at unusually negative potentials that are well within the double layer region.
2. Deposition of copper from acid sulphate baths is severely inhibited at low overpotentials as the primary product cannot readily attain a stable, high lattice coordination state. It is assumed that a partial discharge state is attained, e.g. Cu^{+}_{surf}, which functions (a) as a barrier to further Cu^{2+} reductionat low overpotentials and (b) as a basis for binding many bath additives (A), as surface complexes, $Cu(A)^{+}_{n}$, which inhibit deposition at the interface.
3. There is a low level active state (or site) redox transition, represented here as Cu^{*}/Cu^{+}_{surf}, which occurs with copper in aqueous acid solution at ca. -0.7 ± 0.1 V (SMSE). The latter potential range coincides with the transition from (i) activation to transport controlled plating of copper in additive-free acid copper plating baths, (ii) highly inhibited to rapid plating in the presence of a variety of bath additives, (iii) low to high electrocatalytic activity for a number of reduction reactions at copper in acid solution. One additive, Cl^-, is an exception in that it catalyses, rather than inhibits, plating at low overpotentials; this anion is assumed to interact strongly with Cu^{+}_{surf}, thereby reducing the repulsion barrier ($Cu^{+}_{surf} \leftrightarrow Cu^{2+}_{aq}$) at the interface. The origin of the critical potential at ca. −0.7 V is uncertain; tentatively it is attributed to the redox behaviour of surface copper clusters.

Acknowledgements

This material is based on work supported by Science Foundation Ireland (SFI) under Grant No. 02/INI/1217. The award of postgraduate research studentships by Intel Ireland (AMO'C), SFI (RS) and the Irish Government (IRCSET scheme) (CAB) is acknowledged.

References

1. P.C. Andricacos, *The Electrochem. Soc. Interface* **8** (1999) 32.
2. P.C. Andricacos, C. Uzoh, J.O. Dukovic, J. Horkans and H. Deligianni, *IBM J. Res. Develop.* **42** (1998) 567.
3. M.A. Hussein and J. He, *IEEE Trans. Semiconductor Manuf.* **18** (2005) 69.
4. M. Kang, M.E. Gross and A.A. Gerwirth, *J. Electrochem. Soc.* **150** (2003) 292.
5. T.P. Moffat, D. Wheeler, E.D. Edelstein and D. Josell, *IBM J. Res. Develop.* **49** (2005) 19.
6. M. Kang and A. Gerwirth, *J. Electrochem. Soc.* **150** (2003) 426.
7. L. Oniciu and L. Muresan, *J. Appl. Electrochem.* **21** (1991) 565.
8. D. Stoychev and C. Tsvetanov, *J. Appl. Electrochem.* **26** (1996) 741.
9. J.P. Healy and D. Pletcher, *J. Electroanal. Chem.* **338** (1992) 155.
10. J.J. Kelly, C. Tian and A.C. West, *J. Electrochem. Soc.* **146** (1999) 2540.
11. L. Bonou, M. Eyraud, R. Denoyel and Y. Massiani, *Electrochim. Acta* **47** (2002) 4139.
12. E. Behana, P.F. Mendez, R. Ortega, L. Salgado and G. Trejo, *Electrochim. Acta* **49** (2004) 989.
13. R.E. Reed-Hill and R. Abbaschian, *Physical Metallurgy Principles*, 3rd ed., (PWS – Kent Publishing Co., Boston, 1992), pp. 227–269.
14. D.N. Buckley and S. Ahmed, *Electrochem. Solid State Letts.* **6** (2003) C33.
15. P.W. Atkins, *Physical Chemistry*, 4th ed., (Oxford University Press, Oxford, 1990), pp. 874.
16. L.D. Burke, A.J. Ahern and A.P. O'Mullane, *Gold Bull.* **35** (2002) 3.
17. L.D. Burke, *Gold Bull.* **37** (2004) 125.
18. A.J. Ahern, L.C. Nagle and L.D. Burke, *J. Solid State Electrochem.* **6** (2002) 451.
19. L.D. Burke, L.M. Kinsella and A.M. O'Connell, *Russ. J. Electrochem.* **40** (2004) 1105.

20. L.D. Burke and N.N. Naser, *J. Appl. Electrochem.* **35** (2005) 931.
21. L.D. Burke and J.A. Collins, *J. Appl. Electrochem.* **29** (1999) 1427.
22. L.D. Burke, J.A. Collins and M.A. Murphy, *J. Solid State Electrochem.* **4** (1999) 34.
23. J.J. Kelly and A.C. West, *J. Electrochem. Soc.* **145** (1998) 3472.
24. B.C. Gates, *Catalytic Chemistry* (Wiley, New York, 1992), pp. 352.
25. T. Wolfram and S. Ellialtioglu. *in* J.R. Smith (ed.), 'Theory of Chemisorption', (Springer-Verlag, Berlin, 1980), pp. 150.
26. L. Lloyd, D.E. Ridler and M.V. Twigg. *in* M.V. Twigg (ed.), 'Catalyst Handbook', 2nd edn., (Wolf Publishing, London, 1989), pp. 290.
27. Th Schedel–Niedrig, M. Hävecker, A. Knop-Gericke and R. Schlögl, *Phys. Chem. Chem. Phys.* **2** (2002) 3473.
28. G. Kyriacou and A. Anagnostopoulos, *J. Electroanal. Chem.* **322** (1992) 233.
29. B. Jermann and J. Augustynski, *Electrochim. Acta* **39** (1994) 1891.
30. D. Pletcher and Z. Poorabedi, *Electrochim. Acta* **24** (1979) 1253.
31. W.J. Albery, B.G.D. Haggett, C.P. Jones, M.J. Prichard and L.R. Svanberg, *J. Electroanal. Chem.* **188** (1985) 257.
32. G.E. Dima, A. de C.A. and M.T.M. Koper, *J. Electroanal. Chem.* **554** (2003) 15.
33. T.R. Nolen, *J. Electrochem. Soc.* **135** (1988) 29C.
34. T.I. Quickenden and Q. Xu, *J. Electrochem. Soc.* **143** (1996) 1248.
35. G. Ertl. *in* B.C. Gates and H. Knözinger (eds), 'Advances in Catalysis' 45, (Academic Press, New York, 2000), pp. 49.
36. H.S. Taylor, *Proc. Roy. Soc. Lond. A* **108** (1925) 105.
37. G.A. Somorjai. *in* D.D. Eley, H. Pines and P.B. Weisz (eds), 'Advances in Catalysis' 26, (Academic Press, New York, 1977), pp. 1–68.
38. L.L. Kesmodel and L.M. Falicov, *Solid State Commun* **16** (1975) 1201.
39. A. Henglein, *J. Phys. Chem.* **97** (1993) 5457.
40. L.D. Burke, *Electrochim. Acta* **39** (1994) 1841.
41. D. Pletcher, *J. Appl. Electrochem.* **14** (1984) 403.
42. R.W. Murray. *in* A.J. Bard (ed.), 'Electroanalytical Chemistry' 13, (Dekker, New York, 1984), pp. 191–368.
43. J.O'M. Bockris, A.K.N. Reddy, M. Gamboa-Aldeco, *Modern Electrochemistry*, Vol 2A, 2nd edn. (Kluwer/Plenum, New York, 2000) pp. 1316–1340.
44. R.J. Randler, D.M. Kolb, B.M. Ocko and I.K. Robinson, *Surf. Sci.* **447** (2000) 187.
45. E. Mattson and J.O'M. Bockris, *Trans. Faraday Soc.* **55** (1959) 1586.
46. R.J. Turner and G.R. Johnson, *J. Electrochem. Soc.* **109** (1962) 798.
47. E.E. Farndon, F.C. Walsh and S.A. Campbell, *J. Appl. Electrochem.* **25** (1995) 574.
48. A. Alodan and W. Smyrl, *Electrochim Acta* **44** (1998) 299.
49. A. Szymaszek, J. Biernat and L. Pajdowski, *Electrochim. Acta* **22** (1977) 359.
50. Z. Nagy, J.P. Blaudeau, N.C. Hung, L.A. Curtis and D.J. Zurawski, *J. Electrochem. Soc.* **142** (1995) 87.
51. M. Yokoi, S. Konishi and T. Hayashi, *Denki Kagaku* **52** (1984) 218.
52. J.P. Healy, D. Pletcher and M. Goodenough, *J. Electroanal. Chem.* **338** (1992) 155.
53. S. Goldbach, W. Messing, T. Daenen and F. Lapicque, *Elctrochim. Acta* **44** (1998) 323.
54. V.D. Jovic and B.M. Jovic, *J. Serb. Chem. Soc.* **66** (2001) 935.
55. L. Bonou, M. Eyraud, R. Denoyel and Y. Massiani, *Electrochim. Acta* **47** (2002) 4139.